2nd International Conference on Engineering Optimization
September 6–9, 2010, Lisbon, Portugal

Combining Shape and Structural Optimization for the Design of Morphing Airfoils

Alessandro De Gaspari* and Sergio Ricci†

Dipartimento di Ingegneria Aerospaziale – Politecnico di Milano
Via La Masa 34, 20156 Milano – Italy
e–mail: *degaspari@aero.polimi.it and †sergio.ricci@polimi.it

Abstract

The great interest in developing morphing airfoils is mainly based on their capability to adapt their shape to optimize some specific aircraft performance indices during the mission. Nevertheless, the design of these kind of devices requires the availability of ad-hoc developed procedures able to tackle the conflicting requirements such as the high deformability requested to change the airfoil shape coupled to the load carrying capability. Hence, the design of the external aerodynamic shape and the whole airfoil structure should be simultaneously carried out. This work proposes a compact approach to combine an aero-structural shape optimization, able to determine the most efficient aerodynamic shape which at the same time minimize the requested energy to deform the airfoil skins, with a topology and sizing structural optimization. The link is a compact parametric technique, based on a Class/Shape function transformation method.

Keywords: morphing; parametric shape representation; radial basis functions; non–linear structural analyses; compliant mechanisms.

1 Introduction

The design of aicraft able to adapt their aerodynamic shape, allows to increase the flight envelope to meet design performance constraints at different phases of any mission profile, but in many cases this requires to invent new structural concepts which are strictly related to the currently available technologies. Recent developments in actuation and sensing technology have restored energy in the research of adaptive or morphing aircraft structures. Smart material based technology may be applicable to the design of morphing structures, thus reducing the complexity due to mechanical hinges and numerous moving parts by means of embedded and distributed actuation devices. The synthesis of smart structures can be accomplished by attaching actuators and sensors to conventional structures or by synthesizing composite systems containing several active constituents and using these new materials to build the structures [1]. In this work an alternative approach to obtain the required shape change by efficiently distributing the elastic energy into the optimized structure by means of few actuators is proposed. This approach is based on the distributed compliance concept instead of the distributed actuation one and leads to the compliant structures, that are both flexible and bearing bio–inspired structures. The structure is optimized to spread elastic strain over itself, so that all its elements share the actuator input load and produce the desired effects. In this way, the structural design depends on the choice of the actuation device and produces a structural configuration suitable to host it. The input load can be obtained by using conventional actuation devices or smart materials which are embedded into the structure.

This approach is built-up on the basis of previous experiences in the design and implementation of morphing concepts [2, 3]. The mechanism developed by PoliMI for active camber concept implementation is based on a modification of the original idea proposed by Dr. Monner from DLR [4] and called for sake of simplicity Rotating Ribs (RR) concept. The proposed concept was based on the substitution of the traditional connection between the skin and the ribs, based on rivets, with a discrete number of linear slides which allow the skin to glide over the rib contour. The concept was applied to the Trailing Edge of the airfoil, where upper and lower skins are not rigidly connected each others but they are able to glide into a linear slide bearing. The proposed morphing mechanism can be lodged into a classical control surface, like the main flap of a transport aircraft, as a sort of retrofit, to maximize the aerodynamic lift–to–drag ratio or to optimize the load distribution (load alleviation) during the flight. The natural next step of this morphing concept is the Adaptive Compliant Wing (ACW): the trailing edge rotating

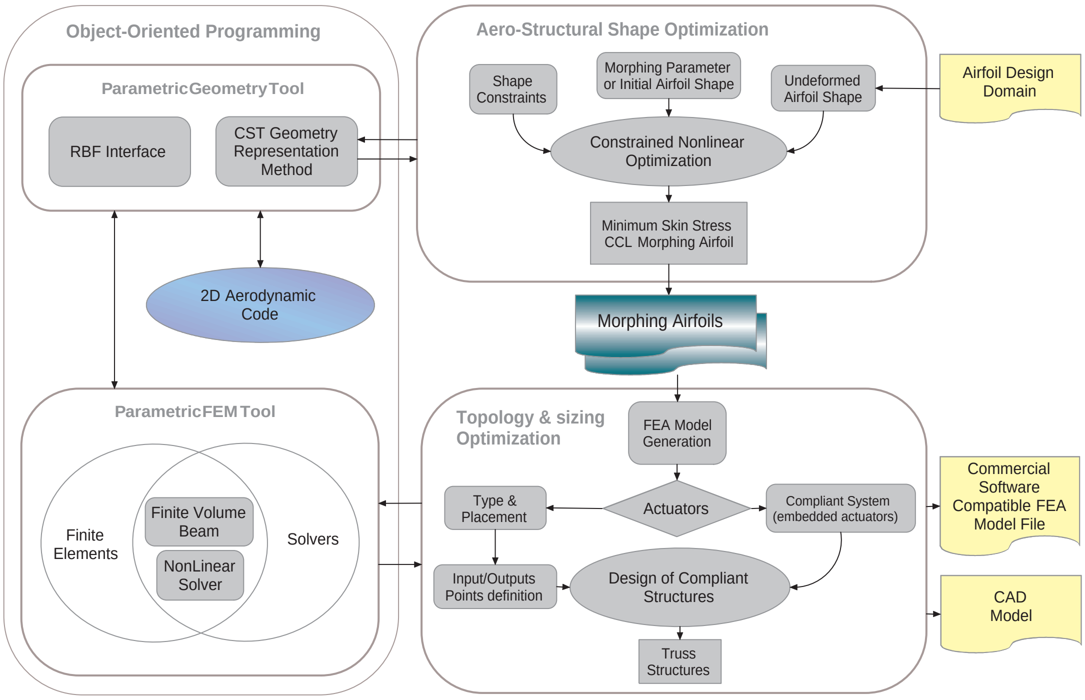

Figure 1: Layout of the proposed approach for the design of morphing airfoils.

ribs are replaced with a single–piece flexible structure able to adapt itself and the corresponding airfoil for matching the desired aerodynamic shape, with the most efficient use of embedded actuators.
One of the most important obstacle in the transition from a conventional control surface to morphing leading or trailing edges is due to the structural contribution of the airfoil skins. Indeed, in the morphing airfoils based on different structural configuration of the rib, the structural contribution of the skin still remains. A wide review of morphing skins concept is presented in [5]. Moreover many studies reported in literature are based on skin made of special active materials who's mechanical characteristics can be tuned, for example, by means of electrical inputs. In the approach here presented an optimization procedure is proposed to determine the most efficient aerodynamic shape which at the same time minimize the requested energy to deform the airfoil skins, so to minimize the power of actuator necessary to control the shape change.

2 An Optimization Procedure Based On a Two Levels Approach

The overall objective of this paper is the development of a procedure for optimal design of morphing airfoils. The procedure shown in Figure 1 is based on a two levels optimization procedure. The definition of morphing airfoil shape changes is strongly influenced by the presence of the airfoil skin, which plays a determinant role in the design of any morphing technique. For this reason the first optimization level described in 4, is coupled to a compact airfoil representation technique (CST), based on the approach proposed by Kulfan in [6], here extended to both leading and trailing edge continuous control surfaces. In this way, an aero–structural shape optimization, mainly focused on the definition of the best airfoil shape variation as the most efficient aerodynamic shape which at the same time minimize axial and bending stresses in the skins, has been implemented. After that, the second optimization level described in 5, based on the synthesis of compliant mechanisms by means of sizing and topology optimization techniques, is adopted to design the best internal structural configuration. This alghoritm runs coupled to an in–house non–linear FEA solver using Finite Volume Beam elements [7].
The whole procedure makes up a specific design tool that can assist engineers in the design of the optimal morphing airfoil.

3 Morphing Airfoil Shape Definition

The starting point of any optimization procedure applied to morphing airfoils requires the definition of the design domain, representing all the possible shapes assumed by the airfoil to satisfy all the aerodynamic requirements. Indeed, the optimal airfoil structure must be able to maintain the configuration that ensures the generation of aerodynamic loads needed for cruising and for maneuvering aircraft. Moreover, the optimal structure must guarantee also a smooth and continuous changes among different external shapes related to variable flight requirements.

One of the main difficulty in approaching the optimization of airfoils is related to how to represent these continuous geometry changes, so to be efficiently implemented into an optimization procedure. Indeed, it must be remembered that the choice of parametrization techniques for geometry representation has enormous impact on the implementation of the optimization problem, directly determining the number of design variables. In particular, in the case of morphing airfoils, a shape function, instead of geometric variables like the rotation angle of conventional control surface rotations, needs to be defined.

The available parameterizations techniques can be grouped into several categories [8]: discrete, polynomial and spline, CAD-based and analytical. The discrete approach uses the grid–point coordinates as design variables: the shape is perturbed by moving individual grid points, thus a smooth geometry is difficult to maintain during the morphing shape changes. Moreover, the number of design variables can become very large and lead to high computational cost.

The use of polynomial representations for shape parameterizations reduces the total number of design variables: the Bezier curve can be described by the same number of control points (design variables) as Bernstein polynomials; the complex curves require a high–degree Bezier form to be approximate, but the higher the degree of a Bezier curve, the greater the roundoff error and the computational cost. Instead, to represent a complex curve, can be used several low–degree Bezier segments covering the entire curve. The resulting piecewise curve is labelled as B–spline. This is a very useful parametric polyline with an important property: each segment is tangent to the previous and following one at its bounding points. In such a ways, moving these points the entire curve keeps its smoothness, but each perturbation affects only one segment.

Instead, to achieve morphing goals, a parameterizations technique that allows to deform the global shape properties of the airfoil without affecting its local regularity, should be found. The analytical approach can be used to introduce a compact formulation based on merging shape function with a baseline shape: the baseline function mathematically defines a variety of basic shape classes, so a complex shape can be represented without breaking the entire curve into several Bezier segments.

3.1 The Class/Shape function Transformation (CST) for Morphing Shape Definition

The technique here proposed for morphing airfoil representation starts from a mathematical formulation based on the analytically function transformation technique, proposed by Kulfan in [9]. This parameterizations technique is well suited to represent the shape changes of morphing airfoils. However in the aerodynamic shape optimizations the geometry changes are very small and they occur with respect to a reference system with origin on the airfoil leading–edge nose; instead, as shown in Figure 2, in the problems related to the morphing the airfoil shape changes with respect its undeformed condition. Therefore an extension of cited technique, that allows to deform the leading–edge, is here proposed.

In CAD applications and computer graphics, Bezier curves are widely used to model smooth curves. The Bezier curve definition is particularly adapt to uniformly approximate continuous functions on the interval $x/c \in [0, 1]$. The Class function/Shape function Transformation (CST) geometry representation method is a powerful application of the generalized Bezier curve definition to represent any aircraft geometries. The class function defines fundamental classes and the shape function defines unique geometric shapes with each class.

The airfoil shape function is decomposed into scalable components by representing the shape function with a Bernstein polynomial. In this way the shape function results a blended function that eliminates slope or curvature discontinuities and can be controlled by scaling different component. The shape function is merged with class function for modeling the leading–edge and the trailing–edge: the airofoil leading–edge nose radius, the trailing–edge thickness and the boat–tail angle are related to the bounding values of the Bezier–based shape function. The approximation curves can be used either to directly form the upper or lower airfoil curves or to generate the mean camber line and airfoil thickness.

The general form of the mathematical expression representing the airfoil geometry is:

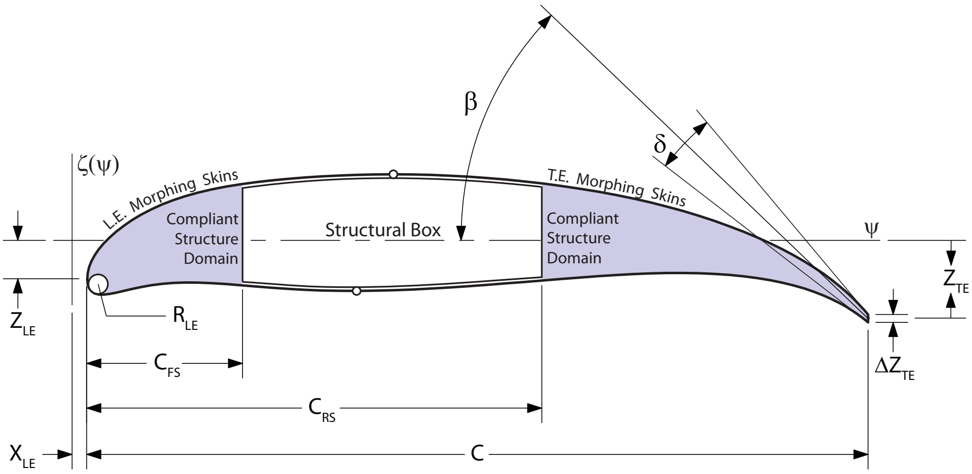

Figure 2: Geometrical parameters adopted for morphing airfoil optimization

$$\zeta(\psi) = C_{N2}^{N1}(\psi)S(\psi) + \psi\zeta_{TE} \tag{1}$$

where $\psi = x/c$, $\zeta = z/c$ are the nondimensional coordinates with respect to airfoil chord c and $\zeta_{TE} = Z_{TE}/c$.
The first term of Eq.(1) is the class function:

$$C_{N2}^{N1}(\psi) \triangleq (C_{LE} + \psi^{N1}) \cdot (1-\psi)^{N2} \tag{2}$$

where C_{LE} is a constant that allows a morphing leading–edge deformation as a vertical translation of the nose. For the sake of brevity, in this paper all of the mathematical steps are not included, but it can be shown how to evaluate C_{LE}. To obtain a nose translation equal to Z_{LE}, C_{LE} must be set according to the following formula: $C_{LE} = \frac{Z_{LE}/c}{A_0}$.
Different exponents ($N1$ and $N2$) in the class function, are used to mathematically define a variety of basic general shapes. In such a ways, round nose, elliptic or minimum drag supersonic biconvex body, as well as rectangle or circular form geometry can be also represented.
The second term is the shape function of selected order n:

$$S(\psi) = \sum_{i=0}^{n} A_i S_i(\psi) \tag{3}$$

where $S_i(\psi) = K_i\psi^i(1-\psi)^{n-i}$ is the Bernstein polynomial component and K_i is the associated binomial coefficient. The coefficients A_i multiply the individual Bernstein polynomial component.
The first and last term of the shape function are determined by imposing boundary conditions on the airfoil shape: they result directly related to the airfoil leading–edge nose radius R_{LE} and trailing–edge boat–tail angle β and thickness ΔZ_{TE} (all of CST method parameters are shown in the figure 2):

$$S(0) = A_0 = \sqrt{2[R_{LE}/c]}, \qquad S(1) = A_n = \frac{\tan\beta + Z_{TE}/c}{C_{LE}+1} \tag{4}$$

Normally, using the CST method to represent an airfoil, the two leading–edge nose radius, corresponding to the upper and lower curve, must be set to the same value. In the problems related to the morphing, a shape deformation corresponding to a leading–edge rotation could lead to an horizontal translation of the nose. The same effect can be reproduced without an airfoil chord reduction by setting different radius values. However, this is the source of a numerical singularity in the camber line curve for $x/c = 0$, thus it is not recommended to apply the corresponding geometry formulation to aerodynamic codes.
The other $n-1$ middle terms in the Eq.(3) neither affect the leading–edge radius nor the trailing–edge angle and can be used to scale the individual Bernstein components. In this way, the perturbation of one of these coefficients spreads on the entire design space of the airfoil maintaining its local smoothness; however the perturbation decreases away from the location of the component peak.

4 Level 1 Optimization Procedure: Aero–Structural Shape Optimization

The initial and target shapes the morphing airfoil must assume, are derived by a first level shape optimization able to define the best airfoil change able to satisfy specifically imposed mission requirements. One of the most important obstacle in the airfoil morphing is due to the structural contribution of the airfoil skin. Indeed, even if almost all the proposed approach for morphing airfoils are based on a different structural configuration of the rib, the structural contribution of the skin still remains. Many studies reported in literature are based on skin made of special active materials who's mechanical characteristics can be tuned, for example, by means of electrical inputs. In the approach here presented the structural configuration adopts classical material skin but the first level optimization procedure is able to define the best morphing shape to minimize the deformation energy of the skin itself and, at the same time, to minimize the power of actuator necessary to control the shape change. This approach is general and can be easly applied to skin made of different kind of material.
The optimization problem formulation is implemented using the compact method reported in the previous section both to compute axial and bending stresses in the skins and to generate the airfoil geometry for the aerodynamic analysis. Nevertheless, the structural and aerodynamic terms must be combined in some way. One simple way to do this is by using a weighted linear combination of the two objectives in a multi–criteria optimization approach. Using appropriate weighting factors, the effect of each term can be tuned in the solution.

The starting point of the first level of the optimization procedure is the compact method reported in the previous section to describe the airfoil geometry. Thanks to this analytical representation technique it results very easy the calculation of the first and second order derivatives, of the airfoil description function, used to compute the length and curvature of airfoil upper, mean and lower surface, i.e.:

$$\mathrm{L}(x) = \int_0^c \sqrt{1 + \left(\frac{dz}{dx}\right)^2}\, dx \tag{5}$$

$$\kappa(x) = \frac{f''(x)}{\left(1 + f'^2\right)^{3/2}}, \tag{6}$$

While the second one is analytically computed, the first one is evaluated semi–analytically. These geometrical quantities are strictly related to the structural properties of the morphing airfoil. For example, the shape change is much more easy if the total length of upper and lower skin surfaces is kept as much constant as possible, so to minimize the axial stresses in the skin that counter react the shape change. Following this idea, it is possible to define a first optimization strategy, here named Constant Cross–section Length (CCL) aiming at the minimization of the maximum axial stress along the skins when they are deformed into the target shape. Nevertheless, the maximum stress consists of two term: the stress due to axial tension or compression σ_{axial} and the stress due to bending σ_{bend}. For the first one, the algorithm computes the length of both undeformed and target airfoil surfaces and estimates the axial stress that is required to stretch or compress the morphing skins. The bending stress is computed by means of the calculation of the curvature difference between the initial and the final shape:

$$\Delta\kappa(l) = \kappa_m\left(x(l)\right) - \kappa_u\left(x(l)\right) \tag{7}$$

where κ_u and κ_m are the curvature functions of the undeformed and morphing surfaces, $x(l)$ is the inverse of normalized arc length function that can be computed starting from the Eq.(5). According to Euler–Bernoulli beam theory, the maximum bending stress along the skin can be calculated from the curvature difference function as:

$$\sigma_{bend} = \frac{Et}{2}\left(\Delta\kappa(l)\right) \tag{8}$$

where E is the Young's Modulus and t is the the skin thickness. Since Eq.(8) is based on the difference between the final and initial curvature distribution, it is general and suitable to compute stress values due to shape changes corresponding to large displacements.

The aerodynamic term of the shape optimization is used to guarantee the morphing airfoil has optimal aerodynamic characteristics at each one of different flight conditions, as also described in [10]. A viscous and subsonic code allows to add the aerodynamic efficiency L/D to the objective function.

After the airfoil CST model has been generated, it is mathematically defined and its shape can be control led. Moreover, to solve the shape optimization problem, the design variables must be defined.

Optimization design variables are the CST method parameters described in 3.1, while optimization fixed parameters are constant values that remain the same during the optimization: they are the front spar position C_{FS} and rear spar position C_{RS} and the desired morphing LE deflection ΔZ_{LE} or TE deflection ΔZ_{TE} with respect to the undeformed ones, as shown in Figure 2. The designer can choose different parameter values to explore different solution space. The optimization algorithm used at this level of the procedure is the Sequential Quadratic Programming (SQP) method. Two different optimization problem for Leading Edge and Trailing Edge are defined and briefly described in the following paragraphs.

4.1 Morphing Leading–Edge CCL Airfoil

The optimization problem can be stated as follows:
Minimize:

$$w_1 \cdot \|z_m(x_{box}) - z_u(x_{box})\|_2^2 \ + \ w_2 \cdot \sigma_{bend} \ + \ w_3 \cdot \frac{1}{L/D} \tag{9}$$

Subject to:

$$\begin{aligned} |L_{LE,\,m} - L_{LE,\,u}| &\leq \Delta L_{LE} \cdot c \\ |A_m - A_u| &\leq \Delta A \cdot A_u \end{aligned}$$

where the first constraint term represents the maximum allowed length variation of the all Leading Edge skin ΔL_{LE} in chord percentage and the second one represents the maximum airfoil area variation ΔA (inflatable term) of the entire airfoil with respect to the undeformed area. w_1, w_2 and w_3 are the weighting terms.

4.2 Morphing Trailing–Edge CCL Airfoil

The optimization problem can be stated as follows:
Minimize:

$$w_1 \cdot \|z_m(x_{box}) - z_u(x_{box})\|_2^2 \ + \ w_2 \cdot (\sigma_{axial} \ + \ \sigma_{bend}) + w_3 \cdot \frac{1}{L/D} \tag{10}$$

Subject to:

$$\begin{aligned} |L_{Up,\,m} - L_{Up,\,u}| &\leq \Delta L_{Up} \cdot c \\ |L_{Low,\,m} - L_{Low,\,u}| &\leq \Delta L_{Low} \cdot c \\ |A_m - A_u| &\leq \Delta A \cdot A_u \end{aligned}$$

where the first two constraint terms represent the maximum allowed length variations of upper ΔL_{Up} and lower ΔL_{Low} surface skins and in chord percentage and the second one represents the same inflatable term of the leading edge problem.
The optimal deformed shapes obtained during the first level optimization procedure will be used as target shapes during the second level optimization so to guarantee the minimum of energy necessary to deform the airfoil.

5 Level 2 Optimization Procedure: Design of Compliant Mechanisms for Morphing Airfoils

The design of shape–adaptable systems in the aeronautical field represents a real challenge because the conflicting requirements of deformability, load–carrying capability and low weight must be conciliate [11]. The discipline that deals with the second two requirements, leads to lightweight structures able to bear external loads, but with a low level of deformability: under certain conditions, minimizing weight is equivalent to maximizing stiffness and this is the basis of structural optimization procedures [12]. Mechanical engineering is the discipline of the conventional mechanisms that are highly movable systems able to carry high loads, but with an intrinsic weight penalization. A third discipline is that of compliant mechanisms which combine deformability and low weight, but they are limited in the load–carrying capability, due to the stress concentration effects in the lumped compliance regions. The whole procedure here presented is based on the *distributed compliance* concept, in which only flexible elements are employed instead of rigid links connected by flexure hinges. In the lumped compliance approach a large–length flexure increases the load–to–weight ratio; by continuing to increase the length up to a solution without rigid parts, the resulting structural configuration approaches compliant systems with distributed compliance. This is a *lightweight* system which has to be optimized to spread elastic strain over the entire structure so that all its elements share the actuator input load to produce large deformation; without stress concentrations it is suitable for high load bearing applications.

The second optimization level employs a topology optimization of Finite Volume Beams (described in the next section) to synthesize distributed compliance structures. In this approach the system configuration is found by allowing a set of connections between a fixed set of nodal points. Continuously varying cross–sectional beam areas can be used as design variables and the topology problem can be also viewed as a sizing problem [13]. Morphing airfoils are loaded by distributed aerodynamic loads so they have to meet deformability and load–carrying requirements in a large number of degrees of freedom. Unlike the typical single–output compliant mechanisms, the airfoil shape control problem has a multiple output nature [14]. The proposed optimization problem aims to optimize compliant structure to trasfer the actuator force to a set of so–called *active points*, placed along the airfoil skin contour, in order to minimize the Least Square Error (LSE) between the deformed curve and the desired morphing shape coming out from the first optimization level:

$$LSE = \frac{1}{n}\sum_{i=1}^{n}\sqrt{(x_{d,i}-x_{m,i})^2+(z_{d,i}-z_{m,i})^2} \tag{11}$$

subject to size, connectivity, stress and node location constraints. In the Eq.(11), n is the number of control points, x_d and z_d are the grid positions computed by the structural analysis, x_m and z_m the corresponding target shape points. This is the so–called *Load Path Representation* method (see [15]) where the single elements are replaced by paths connecting load input and active points, load input and fixed points or fixed points and active points, as topology optimization variables. This method presents three major advantages: it reduces the number of design variables, ensures structural connectivity by excluding infeasible solutions from the design space and it is free of "gray areas" problems, as described in [16]. In the procedure here presented, the load path representation method has been incorporated into a Genetic Algorithm coupled with a non–linear analysis solver and an interface scheme to trasfer aerodynamic loads to the skin structural model.

5.1 Finite Volume Beam Model

The topology optimization approach described in the previous section is based on structural analyses of frames or trusses. Moreover the use of geometrically non–lnear analyses is absolutely essential for mechanism synthesis subject to large displacements [13]. For these reasons, a particular type of beam, usually adopted as deformable connection component in the multibody applications, has been chosen: the Finite Volume C^0 beam [7]. This is a three–node non–linear beam which proved to be intrinsically shear–lock free. The finite–volume approach leads to the collocated evaluation of internal forces and moments, as opposed to usual variational principles which require numerical integration on a one–dimensional domain. The kinematic description of the generalized deformations, the strains and the curvatures, is based on an intrinsic (kinematically exact) formulation of the beam. Every node is characterized by a position vector $\mathbf{x_i}$ and a rotation matrix $\mathbf{R}(\mathbf{g})$ through Gibbs–Rodrigues rotation parameters g. A reference line $\mathbf{p}$ describes the position of an arbitrary point $\mathbf{p}(\epsilon_\mathbf{i})$ on the beam section. Parabolic shape functions are used to interpolate displacements and rotation parameters of the generic point $\mathbf{p}(\mathbf{x_i})$ as functions of those of the reference nodes. The derivatives of the displacements and the rotation parameters at the two collocation points (laid at $\epsilon_i = \pm 1/\sqrt{3}$ to recover the exact static solution) are used to evaluate the strains and the elastic curvatures which are then used to compute the internal forces and moments, balancing the external forces and moments. Being the position of the $i-th$ node $\mathbf{p_i} = \mathbf{x_i} + \mathbf{R}\mathbf{s_i}$, the position of an arbitrary point of the reference line is:

$$\mathbf{p}(\epsilon) = \mathbf{N_i}(\epsilon)(\mathbf{x_i} + \mathbf{R_i}(\mathbf{g}(\epsilon))\mathbf{s_i}) \quad with\ \mathbf{g}(\epsilon) = \mathbf{N_i}\mathbf{g_i} \tag{12}$$

where $\mathbf{N}(\epsilon) = \begin{bmatrix} \mathbf{1/2}\epsilon(\epsilon-\mathbf{1}) & \mathbf{1}-\epsilon^\mathbf{2} & \mathbf{1/2}\epsilon(\epsilon+\mathbf{1}) \end{bmatrix}$ is the parabolic shape functions.

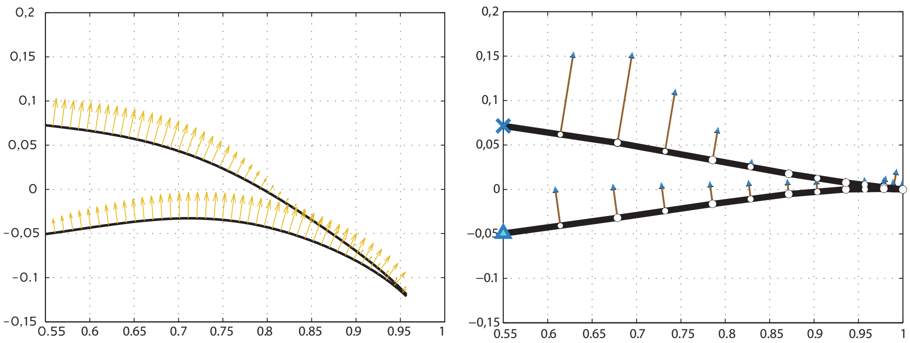

Figure 3: Load transfering from aerodynamic analysis panels to structural nodes.

5.2 Aerodynamic Load Application

Morphing airfoils meet the load–carrying requirement if it is able to adapt its shape and then to maintain it under the external aerodynamic load corresponding to the same flight conditions defined during the first optimization level. The non–linear structural analyses performed during each optimization need the aerodynamic loads are transfered from aerodynamic to structural model. For this purpose the optimization procedure can be run following two different ways:

- The aeordynamic loads are computed for the target shape as a design requirement. The force magnitude is the same, while the direction follows the deformed structure, displacements and rotations of its application points during the non–linear iterations;
- The aerodynamic loads are computed taking into account static aeroelastic considerations during each non–linear iteration.

In the first case the aerodynamic analysis is performed once for all outside the optimization process. If the topology optimization converges, aerodynamic loads correspond to the final shape of the deformed airfoil. In the second one, static aeroelastic loads must achieve the convergence during each non–linear analysis. Non–linear structural analyses comprise two levels of iterative processes: the innermost level for the internal force convergence, while the next one is used to increment the actuator input load until its nominal value. Similary to the general scheme described in [17], static aeroelastic convergence and the non–linear innermost iterations have been efficiently combined. Each iteration is based on nonconverged aeroelastic loads, such that they converge simultaneously. This integrated approach is based on the assumption that the number of iterations required for the aeroelastic convergence should be less than the number of iterations required by the non–linear innermost level.

An interface scheme to exchange these loads between the structural model grids of the airfoil skins and the panels of the 2D aerodynamic analysis model is required. Moreover, if the static aeroelastic effects are considerated, the aerodynamic model must be updated during each non–linear analysis; in order to transfer the displacements from structural to aerodynamic model, the interface must be also applied for all deformed shapes between the undeformed and the target ones. In this case, both the skin beam model and the aerodynamic model represent a one–dimensional domain. As conseguence, two similar representations of the same cover skin geometry must be made perfectly compatible in order to transfer information between them. For this purpose, the Radial Basis Function (RBF) method (see [18] and [19]) is available in the optimization procedure. This method ensure the conservation energy transfer between the fluid and the structure. As shown in Figure 3, aerodynamic loads are distributed along the beam nodes and reduced to lumped forces.

6 Design Example

The described optimization strategy has been applied to the airfoil of the X–DIA wing reference prototype [20]. The wing of this wind–tunnel aeroelastic demonstrator is equipped with an active aeroelastic control based on four conventional control surfaces: two located on the leading edge and the remaining two on the trailing edge. The reference airfoil is the $NACA\,63_2215$, thus the corresponding CST model has been mathematically defined to control its shape. Corresponding morphing leading edge shape has been defined by running the first optimization level, while a very preliminary internal structure of the morphing trailing edge has been also designed.

6.1 Morphing Airfoil Leading Edge

The optimization problem 4.1 has been applied to the X–DIA airfoil in order to shape an optimal morphing leading edge with front spar position C_{FS} at $0.2c$. Figure 4 shows structural results obtained by imposing a deflection value of $\Delta Z_{LE} = -0.05c$, no skin length variation ($\Delta L_{LE} = 1.e{-}5$) corresponding to $\sigma_{axial} = 0$ and an inflatable term ΔA equal to 0.05.

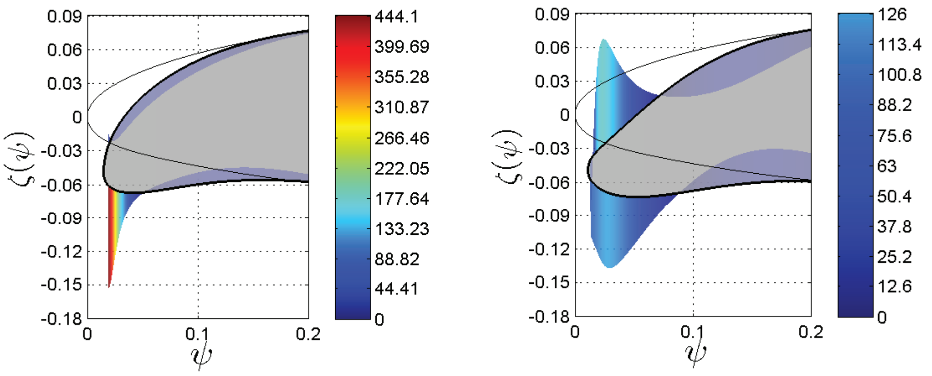

Figure 4: Morphing stresses [MPa] distribution along the Leading Edge skins obtained from the aero–structural and only structural shape optimization.

The aerodynamic benefits of a morphing leading edge are promising. Figure 5 illustrates the comparison between undeformed and morphing airfoil polars. When the leading edge is optimized including aerodynamic considerations, the morphing technology is able to increase the L/D performance over the entire mission. The envelope curve shows a continuous variable geometry allows to optimize the smooth deflection for a wide range of Angle Of Attacks. In this case, the nose shape has been omptimized between 0 to 12 degree AOA and the adaptive leading edge achieves maximum L/D improvement of about 70% compared to the undeformed airfoil.

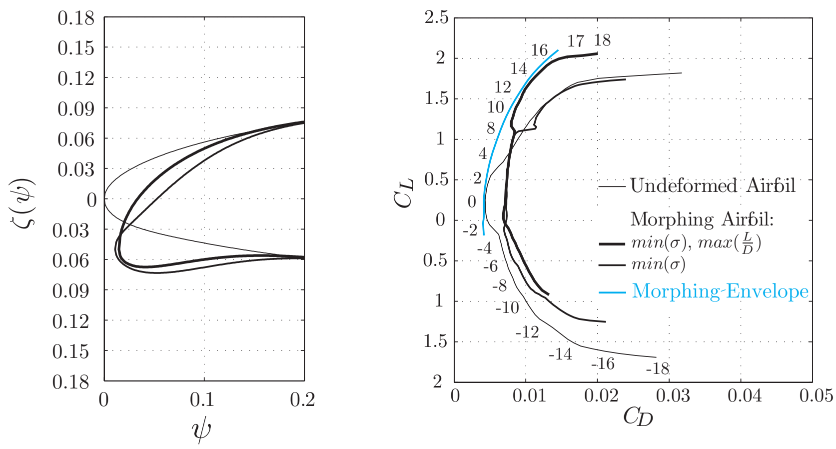

Figure 5: Extension of the airfoil polar with morphing Leading Edge.

It can be noted that the leading edge curvature changes to alleviate the bending stress generated inside the skin and, at the same time, the leading edge radius increases to preserve laminar flow for high lift conditions.

6.2 Morphing Airfoil Trailing Edge

Contrary to the leading edge, in the trailing edge case the skin contour needs to be opened to avoid exceeding strain limits and linear slides must be introduced at the interruption: in the optimization problem 4.2 this aspect can be introduced by opportunely tuning upper and lower skin length constraints. The optimization problem has been applied to the X–DIA airfoil in order to shape an optimal morphing trailing edge with rear spar position C_{RS} at 0.6 c. Figure 6 shows the X–DIA morphing trailing edge structural results obtained by imposing deflection values ΔZ_{TE} of $-0.08\,c$, $-0.10\,c$ and $-0.12\,c$. The upper skin length is set to be constant ($\Delta L_{Up} = 1.e-6$ which leads to $\sigma_{axial} = 0$) according to the CCL concept, while different values of ΔL_{Low} are used; the inflatable term ΔA is equal to 0.05.

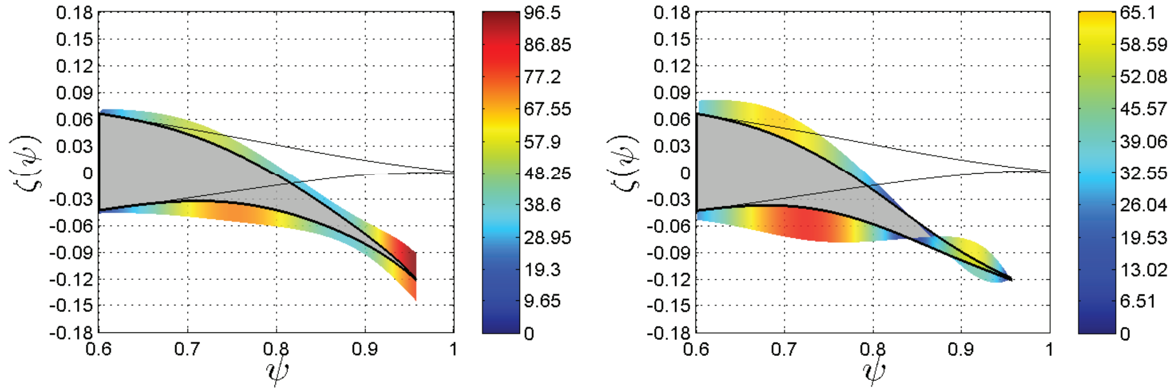

Figure 6: Morphing bending stresses [MPa] distribution along the Trailing Edge skins obtained from the aero–structural shape optimization with different lower skin length constraints.

Although comparisons should be done with respect to the conventional flap, aerodynamic analyses of the morphing trailing edge flap have shown laminar flow is maintened for 75% of the airfoil chord: due to lack of space, in Figure 7 the resulting $C_L - \alpha$ curves for the three different smooth deflections are only illustrated.

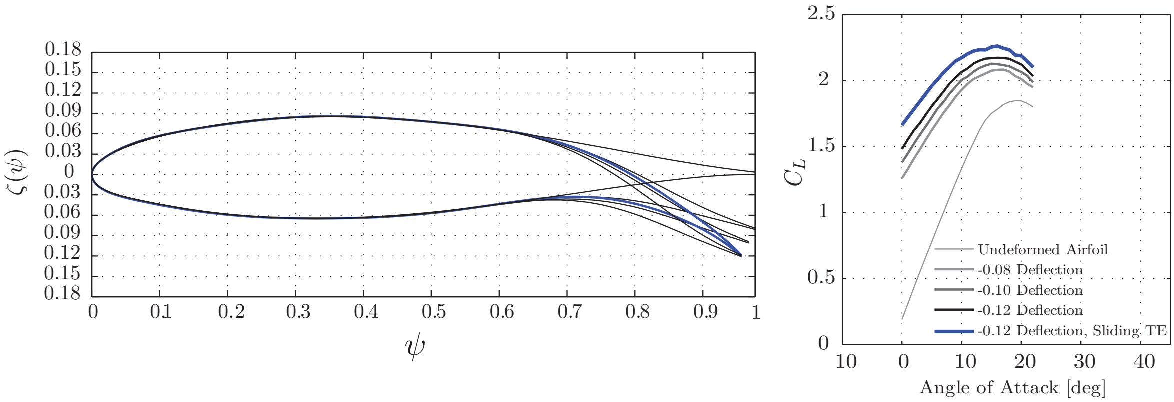

Figure 7: C_l improvement with morphing trailing edge.

The second optimization level has been applied to the morphing trailing edge shape coming out from the first optimization level; lower skin length constraint of the first level has been translated to the second one by applying an horizontal slider instead of a clamp in the finite volume beam model of the lower skin. A preliminar compliant trailing edge solution has been optimized without consider aerodynamic loads; the optimization has synthesized an adaptive compliant structure that requires an actuator force of 200 N to match the morphing shape corresponding to the smooth deflection of $-0.12\,c$. Non–linear analysis normal stress distribution has been computed, as shown in the Figure 8.

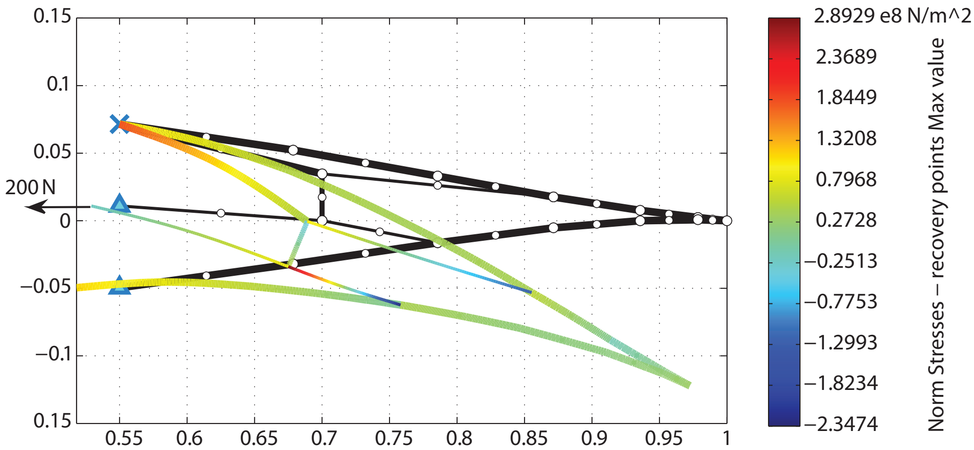

Figure 8: Analysis results of morphing airfoil trailing edge obtained from the described procedure without aerodynamic loads.

Since the second level ran without the aerodynamic load application, this internal structural configuration does not guarantee to meet load–carrying requirement, but it is useful to validate the whole optimization procedure.

7 Conclusions

A two level scheme–based synthesis procedure has been developed for the design of morphing airfoils. With an integrated approach, it allows to combine deformability, load–carrying and low weight requirements of the adaptive rib, dealing, at the same time, with the problem of the connection between the skins and the rib by means of an aero–structural shape optimization. The optimization procedure aims to the synthesis of morphing compliant airfoils by using the LSE as objective function to match the deformed curve, computed by the Finite Volume Beam non–linear analysis, and the target curve coming out from the first optimization level. However, the techniques included in the second optimization level are general and can be used for structural optimization or SISO compliant mechanism synthesis; many different objective function, such as minimizing strain energy or maximizing geometric advantages, can be incorporated in this optimization process. Moreover it adopts a synthesis approach based on GA in which the designer must provide an initial set of design alternatives: a dedicated Graphical User Interface assists the designer at this stage and helps him to understand how the compliant mechanism works by enhancing design intuition.

First optimization level has been applied both to an airfoil leading and trailing edge, showing that the skin contour does not need to be opened in the first case. The complete procedure has been only applied to the trailing edge. A non–linear analysis of the optimized finite volume beam model has been performed: normal stress values along skin elements and the horizontal displacement of the lower slider grid point match the stress values and the skin length variation of the lower skin estimated during the first level. This comparison validates the stress calculation performed by the CST method, in the large displacement case too. More airfoil examples are currently being studied by activating the aerodynamic interface, thus also considering load–carrying capabilities.

Acknowledgements

The authors would like to thank Luca Cavagna for providing an implementation of the Finite Volume Beams which has been embedded with the non–linear FEA solver used in the synthesis of compliant systems.

References

[1] Sater, J. M., Crowe, C. R., Antcliff, R., and Das, A., "Smart Air and Space Structures," *Structures Technology for Future Aerospace Systems*, edited by A. K. Noor and P. Zarchan, Vol. 188, chap. 6, AIAA, 2000, pp. 269–335.

[2] Ricci, S. and Terraneo, M., "Design, Manufacturing and Preliminary Test Results of an Adaptive Wing Camber Model," 47th AIAA/ASME/ASCE/AHS/ASC Structures, Structural Dynamics and Materials (SDM) Conference, Newport, Rhode Island, 1–4 May 2006.

[3] Ricci, S. and Terraneo, M., "Application of MDO techniques to the preliminary design of morphed aircraft," 11th AIAA/ISSMO Multidisciplinary Analysis and Optimization Conference, Portsmouth, Virginia, 6–8 September 2006.

[4] Monner, H. P., "Realization of an Optimized Wing Camber by using Formvariable Flap Structures," *Aerospace Science Technology*, Vol. 5, 2001, pp. 445–455.

[5] Thill, C., Etches, J., Bond, I., Potter, K., and Weaver, P., "Morphing skins," *The Aeronautical Journal*, Vol. 38, No. 10, March 2008.

[6] Kulfan, B. M., "Universal Parametric Geometry Representation Method," *Journal of Aircraft*, Vol. 45, No. 1, January–February 2008.

[7] Ghiringhelli, G. L., Masarati, P., and Mantegazza, P., "Multibody Implementation of Finite Volume C^0 Beams," *AIAA Journal*, Vol. 38, No. 1, January 2000.

[8] Samareh, J. A., "Survey of Shape Parameterization Techniques for High-Fidelity Multidisciplinary Shape Optimization," *AIAA Journal*, Vol. 39, No. 5, May 2001.

[9] Kulfan, B. M., ""Fundamental" Parametric Geometry Representations for Aircraft Component Shapes," 11th AIAA/ISSMO Multidisciplinary Analysis and Optimization Conference, Portsmouth, Virginia, 6 – 8 September 2006.

[10] Secanell, M., Suleman, A., and Gamboa, P., "Design of a Morphing Airfoil Using Aerodynamic Shape Optimization," *AIAA Journal*, Vol. 44, No. 7, July 2006.

[11] Wagg, D., Bond, I., Weaver, P., and Friswell, M., *Adaptive Structures: Engineering Applications*, Wiley & Sons, 2007.

[12] Bindolino, G., Ghiringhelli, G. L., Ricci, S., and Terraneo, M., "Multilevel Structural Optimization for Preliminary Wing-Box Weight Estimation," Vol. 47, AIAA, MarchŰ-April 2010.

[13] Sigmund, O. and Bendsøe, M. P., *Topology Optimization: Theory, Methods and Applications*, Springer, 2003.

[14] Lu, K.-J. and Kota, S., "Design of Compliant Mechanisms for Morphing Structural Shapes," *Journal of Intelligent Material Systems and Structures*, Vol. 14, June 2003, pp. 379–391.

[15] Lu, K.-J. and Kota, S., "An Effective Method of Synthesizing Compliant Adaptive Structures using Load Path Representation," *Journal of Intelligent Material Systems and Structures*, Vol. 16, April 2005, pp. 307–317.

[16] Lu, K.-J. and Kota, S., "Topology and Dimensional Synthesis of Compliant Mechanisms Using Discrete Optimization," *Journal of Mechanical Design*, Vol. 128, September 2006, pp. 1080–1091.

[17] Raveh, D. E., Levy, Y., and Karpel, M., "Structural Optimization Using Computational Aerodynamics," *AIAA Journal*, Vol. 38, No. 10, October 2000.

[18] Beckert, A. and Wendland, H., "Multivariate Interpolation for Fluid–Structure–Interaction Problems Using Radial Basis Functions," *Aerospace Science and Technology*, Vol. 5, 2001, pp. 125–134.

[19] Cavagna, L., *A Multi–fidelity Approach to Computational Aeroelasticity for Fixed Wing Aircraft*, Ph.D. thesis, Dipartimento di Ingegneria Aerospaziale, Politecnico di Milano, 2009.

[20] De Gaspari, A., Ricci, S., Riccobene, L., and Scotti, A., "Active Aeroelastic Control over a Multi-Surface Wing: Modelling and Wind Tunnel Testing," *AIAA Journal*, Vol. 47, No. 9, September 2009.